Mon. Not. R. Astron. Soc. **328,** 815–828 (2001)

Extending Lagrangian perturbation theory to a fluid with velocity dispersion

Masaaki Morita[1,2]★ and Takayuki Tatekawa[3]

[1]*Department of Physics, Ochanomizu University, Ohtsuka, Bunkyo, Tokyo 112-8610, Japan*
[2]*Advanced Research Institute for Science and Engineering, Waseda University, Ohkubo, Shinjuku, Tokyo 169-8555, Japan*
[3]*Department of Physics, Waseda University, Ohkubo, Shinjuku, Tokyo 169-8555, Japan*

Accepted 2001 August 13. Received 2001 July 5; in original form 2001 March 30

ABSTRACT

We formulate a perturbative approximation to gravitational instability, based on Lagrangian hydrodynamics in Newtonian cosmology. We take account of the 'pressure' effect of a fluid, which is kinematically caused by velocity dispersion, to aim the hydrodynamical description beyond shell crossing. Master equations in the Lagrangian description are derived and solved perturbatively up to second order. Then, as an illustration, power spectra of density fluctuations are computed in a one-dimensional model from the Lagrangian approximations and Eulerian linear perturbation theory for comparison. We find that the results by the Lagrangian approximations are different from those by the Eulerian theory in the weakly non-linear regime at scales smaller than the Jeans length. We also show the validity of the perturbative Lagrangian approximations by consulting the difference between the first-order and second-order approximations.

Key words: gravitation – hydrodynamics – instabilities – cosmology: theory – large-scale structure of Universe.

1 INTRODUCTION

It is significant to investigate the evolution of inhomogeneities by gravitational instability in the expanding Universe from the viewpoint of cosmological structure formation. In order to find out how to form cosmic structures via gravitational instability, numerical simulations such as *N*-body simulations have been carried out by several groups (e.g. Miyoshi & Kihara 1975; Hockney & Eastwood 1988; Couchman 1999). Such numerical approaches have given us much useful information about structure formation, but analytical approaches are also needed to obtain a physical understanding of structure formation.

For analytical approaches, one usually treats matter contained in the Universe as a self-gravitating fluid, and considers solving the hydrodynamical equations for the fluid. Since the hydrodynamical equations are generally non-linear, one cannot solve them without making some assumptions or approximations. A conventional approximation is linear perturbation in homogeneous and isotropic universes, based on the Eulerian picture of hydrodynamics (Weinberg 1972; Peebles 1980; Coles & Lucchin 1995; Sahni & Coles 1995). This approach is, by construction, valid only in the linear regime, where the amplitude of density perturbations is much smaller than unity.

For a description beyond the linear regime, Zel'dovich (1970) proposed a new approximation scheme in which perturbations are given as the Lagrangian displacement of fluid flow by an extrapolation of linear perturbation theory. This approximation is known as the Zel'dovich approximation, and has been found to give relatively accurate results and to work better than the Eulerian approximations by comparison with exact solutions (Munshi, Sahni & Starobinsky 1994; Sahni & Shandarin 1996; Yoshisato, Matsubara & Morikawa 1998), in the weakly non-linear regime, where the amplitude of density perturbations becomes comparable to unity. The Zel'dovich approximation has been shown to be a subclass of first-order solutions of perturbation theory in Lagrangian hydrodynamics (Buchert 1989, 1992), and, along this line, higher-order extensions have been developed up to third order (Bouchet et al. 1992; Buchert & Ehlers 1993; Buchert 1994; Bouchet et al. 1995; Catelan 1995; Sasaki & Kasai 1998).

In the Zel'dovich approximation, however, physical singularities called 'shell crossings' inevitably occur. This is a consequence of the fact that a self-gravitating pressureless fluid is taken as a matter model in the approximation. At the epoch beyond shell crossing, the

★E-mail: masaaki@cosmos.phys.ocha.ac.jp

Zel'dovich approximation soon becomes inaccurate because the fluid elements move throughout the directions that are set initially, and then inhomogeneous structures, which are formed compactly once, are dissolved in the approximation scheme. To resolve this problem, some modifications have been proposed, such as the 'truncated Zel'dovich approximation' (Coles, Melott & Shandarin 1993; Melott, Pellman & Shandarin 1994), which is an optimization of the approximation by truncating small-scale fluctuations, and the 'adhesion approximation' (Gurbatov, Saichev & Shandarin 1989), where an artificial viscosity is introduced. These modifications eliminate the shortcomings of the Zel'dovich approximation, and the modified approximations provide excellent results compared with *N*-body simulations in some cases. However, the physical grounds of the modifications are not clear.

To have more well-founded approximations from a physical point of view, we need to study the gravitational instability of pressureless matter beyond shell crossing. Buchert & Domínguez (1998) have examined this issue, starting from the collisionless Boltzmann equation, which is usually applied to stellar systems (e.g. Binney & Tremaine 1987). They argued that the effect of velocity dispersion will be significant beyond shell crossing, and if the velocity dispersion is approximately isotropic, it yields pressure-like or viscosity terms. This implies that the gravitational instability of pressureless matter beyond shell crossing can be described effectively by hydrodynamic equations for a fluid with pressure-like force.

Following this view, Adler & Buchert (1999) have proposed a reformulation of the Lagrangian perturbation theory by taking account of the pressure effect. They derived first-order perturbation equations in the Lagrangian coordinates under the assumption that the pressure is a function of only mass density. They did not, however, present solutions of the perturbation equations or analyse the evolution of density perturbations with the solutions. One may expect the reformulation to extend the regions that can be described by analytical approximations, but this should be confirmed by a concrete illustration. The aim of this paper is to show how the reformulation gives a description of gravitational instability by solving perturbation equations and illustrating the behaviour of density perturbations.

In this paper, we derive and solve the Lagrangian perturbation equations with pressure up to second order, assuming a polytropic equation of state. We adopt the method of Fourier transformation for the solutions and then will see mode couplings in the Lagrangian Fourier space in the second-order solutions. In particular, we obtain the explicit form of the second-order solutions in the case $P \propto \rho^{4/3}$, where P and ρ are pressure and mass density, respectively. Moreover, as an illustration of the formulation, power spectra of density fluctuations are computed in a one-dimensional model from the Lagrangian approximations for the case $P \propto \rho^{4/3}$, and are compared with the results by the Eulerian linear perturbation theory to clarify the difference between them. We also compare the first-order and second-order Lagrangian approximations to examine the validity of the approximation scheme.

This paper is organized as follows. In Section 2 we present the basic equations of our method. Starting from the hydrodynamical equations, we derive master equations of the Lagrangian perturbation theory with the pressure effect. In Section 3 we obtain perturbation equations by expanding the master equations up to second order, and solve them via Fourier transformation. Section 4 gives illustrative examples of the computation of density perturbations by the Lagrangian and the Eulerian approximations in a one-dimensional model. Showing power spectra of density perturbations, we discuss the differences among the approximations. Section 5 contains concluding remarks.

2 BASIC EQUATIONS

We begin with the basic equations of cosmological hydrodynamics for a self-gravitating fluid with energy density ρ and 'pressure' P. In coordinates $\boldsymbol{x} \equiv \boldsymbol{r}/a$ comoving with cosmic expansion, they are

$$\frac{\partial \rho}{\partial t} + 3\frac{\dot{a}}{a}\rho + \frac{1}{a}\nabla_{\boldsymbol{x}} \cdot (\rho \boldsymbol{v}) = 0, \tag{1}$$

$$\frac{\partial \boldsymbol{v}}{\partial t} + \frac{\dot{a}}{a}\boldsymbol{v} + \frac{1}{a}(\boldsymbol{v} \cdot \nabla_{\boldsymbol{x}})\boldsymbol{v} = \boldsymbol{g} - \frac{1}{\rho a}\nabla_{\boldsymbol{x}} P, \tag{2}$$

$$\nabla_{\boldsymbol{x}} \times \boldsymbol{g} = 0, \tag{3}$$

$$\nabla_{\boldsymbol{x}} \cdot \boldsymbol{g} = -4\pi G a(\rho - \rho_{\mathrm{b}}), \tag{4}$$

where $a = a(t)$ is the cosmic scalefactor, $\rho_{\mathrm{b}} = \rho_{\mathrm{b}}(t)$ is the energy density of a homogeneous and isotropic (background) universe, and $\boldsymbol{v}$ and $\boldsymbol{g}$ represent respectively the velocity field and the gravitational field strength due to the presence of an inhomogeneity, and thus may be called the 'peculiar velocity field' and 'peculiar gravitational field'. The 'pressure' that we take into account here is the kinematical one due to the occurrence of velocity dispersion beyond shell crossing of dust flow, as stated by Buchert & Domínguez (1998), rather than the thermodynamical one. Thus equation (2) is close to the Jeans equation, which is obtained by taking moments of the collisionless Boltzmann equation (e.g. Binney & Tremaine 1987).

In a Lagrangian description of hydrodynamics, using the time derivative along the fluid flow,

$$\frac{\mathrm{d}}{\mathrm{d}t} \equiv \frac{\partial}{\partial t} + \frac{1}{a}(\boldsymbol{v} \cdot \nabla_{\boldsymbol{x}}),$$

equations (1) and (2) are rewritten as

$$\frac{\mathrm{d}\rho}{\mathrm{d}t} + 3\frac{\dot{a}}{a}\rho + \frac{\rho}{a}(\nabla_{\boldsymbol{x}} \cdot \boldsymbol{v}) = 0, \tag{5}$$

$$\frac{\mathrm{d}\boldsymbol{v}}{\mathrm{d}t} + \frac{\dot{a}}{a}\boldsymbol{v} = \boldsymbol{g} - \frac{1}{\rho a}\nabla_{\boldsymbol{x}} P. \tag{6}$$

The coordinates $\boldsymbol{x}$ of the trajectories of the fluid elements are expressed by Lagrangian coordinates $\boldsymbol{q}$, defined by the initial values of the coordinates $\boldsymbol{x}$, in the form

$$\boldsymbol{x} = \boldsymbol{q} + \boldsymbol{s}(\boldsymbol{q}, t), \tag{7}$$

where $\boldsymbol{q}$ and $\boldsymbol{s}$ represent the background Hubble flow and the deviation of the flow from the background, respectively. The continuity equation (5) is then exactly solved as

$$\rho = \rho_{\mathrm{b}} J^{-1} \tag{8}$$

or equivalently for density contrast $\delta \equiv (\rho - \rho_{\mathrm{b}})/\rho_{\mathrm{b}}$ as

$$\delta = J^{-1} - 1, \tag{9}$$

where $J \equiv \det(\partial x_i/\partial q_j) = \det(\delta_{ij} + \partial s_i/\partial q_j)$ is the Jacobian of the transformation $\boldsymbol{x} \rightarrow \boldsymbol{q}$. The peculiar velocity is written by definition as $\boldsymbol{v} = a\dot{\boldsymbol{s}}$, and from equation (2) the peculiar gravitational field becomes

$$\boldsymbol{g} = a\left(\ddot{\boldsymbol{s}} + 2\frac{\dot{a}}{a}\dot{\boldsymbol{s}} - \frac{1}{a^2}\frac{\mathrm{d}P}{\mathrm{d}\rho}J^{-1}\nabla_{\boldsymbol{x}} J\right),$$

where an overdot $(\cdot)$ denotes $\mathrm{d}/\mathrm{d}t$. Note that the square of the 'sound speed', $\mathrm{d}P/\mathrm{d}\rho$, is a function of ρ, and can be written in terms of $\boldsymbol{s}$ by using equation (8) if an equation of state is provided. Now all the physical quantities are found to be written in terms of $\boldsymbol{s}$, and it remains only to find solutions for $\boldsymbol{s}$. We obtain the following master equations for $\boldsymbol{s}$ from equations (3) and (4):

$$\nabla_{\boldsymbol{x}} \times \left(\ddot{\boldsymbol{s}} + 2\frac{\dot{a}}{a}\dot{\boldsymbol{s}}\right) = 0, \tag{10}$$

$$\nabla_{\boldsymbol{x}} \cdot \left(\ddot{\boldsymbol{s}} + 2\frac{\dot{a}}{a}\dot{\boldsymbol{s}} - \frac{1}{a^2}\frac{\mathrm{d}P}{\mathrm{d}\rho}J^{-1}\nabla_{\boldsymbol{x}} J\right) = -4\pi G\rho_{\mathrm{b}}(J^{-1} - 1). \tag{11}$$

The relation between $\nabla_{\boldsymbol{x}}$ and $\nabla_{\boldsymbol{q}} \equiv \partial/\partial\boldsymbol{q}$ is obtained from equation (7) as

$$\frac{\partial}{\partial q_i} = \frac{\partial x_j}{\partial q_i}\frac{\partial}{\partial x_j} = \left(\delta_{ji} + \frac{\partial s_j}{\partial q_i}\right)\frac{\partial}{\partial x_j} = \frac{\partial}{\partial x_i} + \frac{\partial s_j}{\partial q_i}\frac{\partial}{\partial x_j}. \tag{12}$$

Using this equation iteratively, we have

$$\frac{\partial}{\partial x_i} = \frac{\partial}{\partial q_i} - \frac{\partial s_j}{\partial q_i}\frac{\partial}{\partial x_j} = \frac{\partial}{\partial q_i} - \frac{\partial s_j}{\partial q_i}\left(\frac{\partial}{\partial q_j} - \frac{\partial s_k}{\partial q_j}\frac{\partial}{\partial x_k}\right) = \frac{\partial}{\partial q_i} - \frac{\partial s_j}{\partial q_i}\frac{\partial}{\partial q_j} + \frac{\partial s_j}{\partial q_i}\frac{\partial s_k}{\partial q_j}\frac{\partial}{\partial x_k} = \cdots. \tag{13}$$

The treatment is fully non-linear and exact so far. Combining equations (10), (11) and (13), in principle we can obtain perturbative solutions for $\boldsymbol{s}$ up to any order. It should be emphasized that density ρ is treated non-perturbatively because of equation (8), even if solutions for $\boldsymbol{s}$ are obtained in a perturbative manner.

3 PERTURBATIVE APPROACH IN LAGRANGIAN COORDINATES

3.1 Derivation of perturbation equations

Let us proceed to a perturbative approach in the Lagrangian description. We write the displacement vector $\boldsymbol{s}$ in the perturbative form $\boldsymbol{s} = \boldsymbol{s}^{(1)} + \boldsymbol{s}^{(2)} + \cdots$. Superscripts (1) and (2) denote first-order and second-order quantities in the perturbative expansion with respect to the amplitude ϵ of primordial fluctuations. We make the perturbative expansion only for $\boldsymbol{s}$, and ρ is not expanded. Then we may expect a relatively accurate description for ρ by this formulation, even in the non-linear regime. In the perturbative expansion, equation (10) gives, to first order,

$$\nabla_{\boldsymbol{q}} \times \left(\ddot{\boldsymbol{s}}^{(1)} + 2\frac{\dot{a}}{a}\dot{\boldsymbol{s}}^{(1)}\right) = 0, \tag{14}$$

and, to second order,

$$\left[\nabla_{\boldsymbol{q}} \times \left(\ddot{\boldsymbol{s}}^{(2)} + 2\frac{\dot{a}}{a}\dot{\boldsymbol{s}}^{(2)}\right)\right]_i = \epsilon_{ijk} s^{(1)}_{\ell,j}\left(\ddot{s}^{(1)}_{k,\ell} + 2\frac{\dot{a}}{a}\dot{s}^{(1)}_{k,\ell}\right), \tag{15}$$

where $(\cdot)_{,i}$ denotes $\partial/\partial q_i$.

Next we consider equation (11). The Jacobian J is expanded as

$$J = 1 + \nabla_{\boldsymbol{q}} \cdot \boldsymbol{s}^{(1)} + \nabla_{\boldsymbol{q}} \cdot \boldsymbol{s}^{(2)} + \frac{1}{2}\left[(\nabla_{\boldsymbol{q}} \cdot \boldsymbol{s}^{(1)})^2 - s^{(1)}_{i,j} s^{(1)}_{j,i}\right] + O(\epsilon^3),$$

and then the square of the 'sound speed', $\mathrm{d}P/\mathrm{d}\rho$, can be written as

$$\frac{\mathrm{d}P}{\mathrm{d}\rho}(\rho) = \frac{\mathrm{d}P}{\mathrm{d}\rho}(\rho_{\mathrm{b}}) - \frac{\mathrm{d}^2P}{\mathrm{d}\rho^2}(\rho_{\mathrm{b}})\rho_{\mathrm{b}} \nabla_{\boldsymbol{q}} \cdot \boldsymbol{s}^{(1)} + O(\epsilon^2).$$

Thus we obtain, to first order,

$$\nabla_{\boldsymbol{q}} \cdot \left[\ddot{\boldsymbol{s}}^{(1)} + 2\frac{\dot{a}}{a}\dot{\boldsymbol{s}}^{(1)} - \frac{1}{a^2}\frac{\mathrm{d}P}{\mathrm{d}\rho}(\rho_{\mathrm{b}})\nabla_{\boldsymbol{q}}(\nabla_{\boldsymbol{q}} \cdot \boldsymbol{s}^{(1)})\right] = 4\pi G\rho_{\mathrm{b}} \nabla_{\boldsymbol{q}} \cdot \boldsymbol{s}^{(1)}, \tag{16}$$

and, to second order,

$$\begin{aligned}
&\ddot{s}^{(2)}_{i,i} + 2\frac{\dot{a}}{a}\dot{s}^{(2)}_{i,i} - \frac{1}{a^2}\frac{\mathrm{d}P}{\mathrm{d}\rho}(\rho_{\mathrm{b}})\nabla^2_{\boldsymbol{q}} s^{(2)}_{i,i} - s^{(1)}_{j,i}\left(\ddot{s}^{(1)}_{i,j} + 2\frac{\dot{a}}{a}\dot{s}^{(1)}_{i,j}\right) + \frac{1}{a^2}\frac{\mathrm{d}P}{\mathrm{d}\rho}(\rho_{\mathrm{b}})(s^{(1)}_{i,ij}\nabla^2_{\boldsymbol{q}} s^{(1)}_{j} + s^{(1)}_{i,jk}s^{(1)}_{j,ik} + s^{(1)}_{i,j}\nabla^2_{\boldsymbol{q}} s^{(1)}_{j,i} + 2s^{(1)}_{i,j}s^{(1)}_{k,kij}) \\
&\quad + \frac{1}{a^2}\frac{\mathrm{d}^2P}{\mathrm{d}\rho^2}(\rho_{\mathrm{b}})\rho_{\mathrm{b}}\left(s^{(1)}_{i,i}\nabla^2_{\boldsymbol{q}} s^{(1)}_{j,j} + s^{(1)}_{i,ik}s^{(1)}_{j,jk}\right) = 4\pi G\rho_{\mathrm{b}}\left[s^{(2)}_{i,i} - \frac{1}{2}(s^{(1)}_{i,i})^2 - \frac{1}{2}s^{(1)}_{i,j}s^{(1)}_{j,i}\right].
\end{aligned} \tag{17}$$

In order to solve the perturbation equations, it is convenient to decompose $\boldsymbol{s}^{(1)}$ and $\boldsymbol{s}^{(2)}$ into longitudinal and transverse parts in the form

$$\boldsymbol{s}^{(1)} = \nabla_{\boldsymbol{q}} S + \boldsymbol{S}^{\mathrm{T}}, \qquad \boldsymbol{s}^{(2)} = \nabla_{\boldsymbol{q}} \zeta + \boldsymbol{\zeta}^{\mathrm{T}},$$

where S and ζ are respectively first-order and second-order scalar functions, and $\boldsymbol{S}^{\mathrm{T}}$ and $\boldsymbol{\zeta}^{\mathrm{T}}$ satisfy $\nabla_{\boldsymbol{q}} \cdot \boldsymbol{S}^{\mathrm{T}} = 0$ and $\nabla_{\boldsymbol{q}} \cdot \boldsymbol{\zeta}^{\mathrm{T}} = 0$. To note their physical meanings, the first-order longitudinal and transverse parts are related to linear density and vortical perturbations, respectively. At the second-order level, however, such a simple interpretation of the perturbation modes no longer holds. The first-order perturbation equations (14) and (16) then become

$$\nabla_{\boldsymbol{q}} \times \left(\ddot{\boldsymbol{S}}^{\mathrm{T}} + 2\frac{\dot{a}}{a}\dot{\boldsymbol{S}}^{\mathrm{T}}\right) = 0, \tag{18}$$

$$\nabla^2_{\boldsymbol{q}}\left[\ddot{S} + 2\frac{\dot{a}}{a}\dot{S} - 4\pi G\rho_{\mathrm{b}}S - \frac{1}{a^2}\frac{\mathrm{d}P}{\mathrm{d}\rho}(\rho_{\mathrm{b}})\nabla^2_{\boldsymbol{q}} S\right] = 0. \tag{19}$$

Under some adequate boundary conditions, these can be reduced to

$$\ddot{\boldsymbol{S}}^{\mathrm{T}} + 2\frac{\dot{a}}{a}\dot{\boldsymbol{S}}^{\mathrm{T}} = 0, \tag{20}$$

$$\ddot{S} + 2\frac{\dot{a}}{a}\dot{S} - 4\pi G\rho_{\mathrm{b}}S - \frac{1}{a^2}\frac{\mathrm{d}P}{\mathrm{d}\rho}(\rho_{\mathrm{b}})\nabla^2_{\boldsymbol{q}} S = 0, \tag{21}$$

which are obtained by Adler & Buchert (1999).

The second-order perturbation equations (15) and (17) are also rewritten in terms of the longitudinal and transverse parts. Equation (15) reads

$$\left[\nabla_{\boldsymbol{q}} \times \left(\ddot{\boldsymbol{\zeta}}^{\mathrm{T}} + 2\frac{\dot{a}}{a}\dot{\boldsymbol{\zeta}}^{\mathrm{T}}\right)\right]_i = 4\pi G\rho_{\mathrm{b}}\epsilon_{ijk}S^{\mathrm{T}}_{\ell,j}S_{,k\ell} + \frac{1}{a^2}\frac{\mathrm{d}P}{\mathrm{d}\rho}(\rho_{\mathrm{b}})\epsilon_{ijk}(S_{,\ell j} + S^{\mathrm{T}}_{\ell,j})\nabla^2_{\boldsymbol{q}} S_{,k\ell}. \tag{22}$$

The curl of this equation gives

$$-\nabla^2_{\boldsymbol{q}}\left(\ddot{\boldsymbol{\zeta}}^{\mathrm{T}} + 2\frac{\dot{a}}{a}\dot{\boldsymbol{\zeta}}^{\mathrm{T}}\right) = \boldsymbol{Q}^{\mathrm{T}}(\boldsymbol{q}, t), \tag{23}$$

where $\boldsymbol{Q}^{\mathrm{T}}$ is a source term, which is quadratic with respect to the first-order perturbations, of the form

$$\begin{aligned}
Q^{\mathrm{T}}_i(\boldsymbol{q}, t) \equiv\ & 4\pi G\rho_{\mathrm{b}}(S^{\mathrm{T}}_{j,ik}S_{,jk} + S^{\mathrm{T}}_{j,i}\nabla^2_{\boldsymbol{q}} S_{,j} - \nabla^2_{\boldsymbol{q}} S^{\mathrm{T}}_{j}S_{,ij} - S^{\mathrm{T}}_{j,k}S_{,ijk}) + \frac{1}{a^2}\frac{\mathrm{d}P}{\mathrm{d}\rho}(\rho_{\mathrm{b}})(S_{,ijk}\nabla^2_{\boldsymbol{q}} S_{,jk} + S_{,ij}\nabla^2_{\boldsymbol{q}}\nabla^2_{\boldsymbol{q}} S_{,j} - \nabla^2_{\boldsymbol{q}} S_{,j}\nabla^2_{\boldsymbol{q}} S_{,ij} - S_{,jk}\nabla^2_{\boldsymbol{q}} S_{,ijk}) \\
&+ \frac{1}{a^2}\frac{\mathrm{d}P}{\mathrm{d}\rho}(\rho_{\mathrm{b}})(S^{\mathrm{T}}_{j,ik}\nabla^2_{\boldsymbol{q}} S_{,jk} + S^{\mathrm{T}}_{j,i}\nabla^2_{\boldsymbol{q}}\nabla^2_{\boldsymbol{q}} S_{,j} - \nabla^2_{\boldsymbol{q}} S^{\mathrm{T}}_{j}\nabla^2_{\boldsymbol{q}} S_{,ij} - S^{\mathrm{T}}_{j,k}\nabla^2_{\boldsymbol{q}} S_{,ijk}).
\end{aligned}$$

Equation (17) becomes

$$\nabla^2_{\boldsymbol{q}}\left[\ddot{\zeta} + 2\frac{\dot{a}}{a}\dot{\zeta} - 4\pi G\rho_{\mathrm{b}}\zeta - \frac{1}{a^2}\frac{\mathrm{d}P}{\mathrm{d}\rho}(\rho_{\mathrm{b}})\nabla^2_{\boldsymbol{q}}\zeta\right] = Q(\boldsymbol{q}, t), \tag{24}$$

where

$$Q(\boldsymbol{q},t) \equiv 2\pi G\rho_{\rm b}[S_{,ij}S_{,ij} - (\nabla_{\boldsymbol{q}}^2 S)^2] - \frac{1}{a^2}\frac{{\rm d}P}{{\rm d}\rho}(\rho_{\rm b})(\nabla_{\boldsymbol{q}}^2 S_{,i}\nabla_{\boldsymbol{q}}^2 S_{,i} + S_{,ijk}S_{,ijk} + 2S_{,ij}\nabla_{\boldsymbol{q}}^2 S_{,ij}) - \frac{1}{a^2}\frac{{\rm d}^2 P}{{\rm d}\rho^2}(\rho_{\rm b})\rho_{\rm b}(\nabla_{\boldsymbol{q}}^2 S\nabla_{\boldsymbol{q}}^2\nabla_{\boldsymbol{q}}^2 S + \nabla_{\boldsymbol{q}}^2 S_{,i}\nabla_{\boldsymbol{q}}^2 S_{,i})$$
$$- \frac{1}{a^2}\frac{{\rm d}P}{{\rm d}\rho}(\rho_{\rm b})(S_{,ij}\nabla_{\boldsymbol{q}}^2 S_{i,j}^{\rm T} + 2S_{,ijk}S_{i,jk}^{\rm T} + \nabla_{\boldsymbol{q}}^2 S_{,i}\nabla_{\boldsymbol{q}}^2 S_i^{\rm T} + 2\nabla_{\boldsymbol{q}}^2 S_{,ij}S_{i,j}^{\rm T}) - 2\pi G\rho_{\rm b}S_{i,j}^{\rm T}S_{j,i}^{\rm T} - \frac{1}{a^2}\frac{{\rm d}P}{{\rm d}\rho}(\rho_{\rm b})(S_{i,j}^{\rm T}\nabla_{\boldsymbol{q}}^2 S_{j,i}^{\rm T} + S_{i,jk}^{\rm T}S_{j,ik}^{\rm T}).$$

We can easily confirm that equations (23) and (24) are consistent with the second-order perturbation equations obtained by Sasaki & Kasai (1998) for the pressureless case.

3.2 Solutions of perturbation equations

Here we solve the perturbation equations in the presence of a pressure effect. We assume that the background universe is a spatially flat one with $a(t) = t^{2/3}$ and $\rho_{\rm b} = 1/(6\pi G t^2) \propto a^{-3}$ for simplicity. The first-order perturbation equation (20) for the transverse part has the same form as in the pressureless case. Thus we immediately find the solutions

$$\boldsymbol{S}^{\rm T} \propto \text{constant},\ \ t^{-1/3}. \tag{25}$$

For the longitudinal part, the Fourier transform of equation (21) with respect to the Lagrangian coordinates yields

$$\ddot{\hat{S}} + 2\frac{\dot{a}}{a}\dot{\hat{S}} - 4\pi G\rho_{\rm b}\hat{S} + \frac{1}{a^2}\frac{{\rm d}P}{{\rm d}\rho}(\rho_{\rm b})|\boldsymbol{K}|^2\hat{S} = 0, \tag{26}$$

where $\hat{(\ )}$ denotes a Fourier component, and $\boldsymbol{K}$ is a wavevector associated with the Lagrangian coordinates $\boldsymbol{q}$. It should be noted that the form of equation (26) is similar to that of an equation for the density contrast $\delta_{\rm lin}$ in the Eulerian linear theory. It reads

$$\frac{\partial^2\delta_{\rm lin}(\boldsymbol{k},t)}{\partial t^2} + 2\frac{\dot{a}}{a}\frac{\partial\delta_{\rm lin}(\boldsymbol{k},t)}{\partial t} - 4\pi G\rho_{\rm b}\delta_{\rm lin}(\boldsymbol{k},t) + \frac{1}{a^2}\frac{{\rm d}P}{{\rm d}\rho}(\rho_{\rm b})|\boldsymbol{k}|^2\delta_{\rm lin}(\boldsymbol{k},t) = 0, \tag{27}$$

where $\boldsymbol{k}$ denotes a wavevector associated with the Eulerian coordinates $\boldsymbol{x}$. As an example, assuming a polytropic equation of state $P = \kappa\rho^\gamma$ with a constant κ and a polytropic index γ, the solutions of equation (27) are (Weinberg 1972)

$$\delta_{\rm lin}(\boldsymbol{k},t) \propto \begin{cases} t^{-1/6}J_{\pm\nu}(A|\boldsymbol{k}|t^{-\gamma+4/3}) & \text{for} \quad \gamma \neq \frac{4}{3}, \\ t^{-1/6\pm\sqrt{25/36-B|\boldsymbol{k}|^2}} & \text{for} \quad \gamma = \frac{4}{3}, \end{cases} \tag{28}$$

where $\nu = 5/(8-6\gamma)$, $J_{\pm\nu}$ is the Bessel function of order $\pm\nu$, and

$$A \equiv \frac{3\sqrt{\kappa\gamma}(6\pi G)^{(1-\gamma)/2}}{|4-3\gamma|}, \qquad B \equiv \frac{4}{3}\kappa(6\pi G)^{-1/3}.$$

Note that the above solutions include wavenumbers of fluctuations, whereas the solutions for the pressureless matter do not. We then find solutions of equation (26) with the help of the known results for the density contrast in the Eulerian linear theory. Hence, in the case of the polytropic equation of state $P = \kappa\rho^\gamma$ and if $\nu = 5/(8-6\gamma)$ is not an integer, we obtain general solutions for $\hat{S}(\boldsymbol{K},t)$ as

$$\hat{S}(\boldsymbol{K},t) = D^+(\boldsymbol{K},t)C^+(\boldsymbol{K}) + D^-(\boldsymbol{K},t)C^-(\boldsymbol{K}), \tag{29}$$

where $D^{\pm}(\boldsymbol{K},t)$ are given, by replacing $\boldsymbol{k}$ with $\boldsymbol{K}$ in equation (28), in the form

$$D^{\pm}(\boldsymbol{K},t) = \begin{cases} t^{-1/6}J_{\pm\nu}(A|\boldsymbol{K}|t^{-\gamma+4/3}) & \text{for} \quad \gamma \neq \frac{4}{3}, \\ t^{-1/6\pm\sqrt{25/36-B|\boldsymbol{K}|^2}} & \text{for} \quad \gamma = \frac{4}{3}, \end{cases} \tag{30}$$

and $C^{\pm}(\boldsymbol{K})$ are determined by the initial conditions. Notice that $\boldsymbol{K}$ is the Lagrangian wavenumber, which is different from the Eulerian wavenumber $\boldsymbol{k}$.

Next we consider solutions of the second-order perturbation equations (23) and (24). The Fourier transformation of equations (23) and (24) gives

$$|\boldsymbol{K}|^2\left(\ddot{\hat{\boldsymbol{\xi}}}^{\rm T} + 2\frac{\dot{a}}{a}\dot{\hat{\boldsymbol{\xi}}}^{\rm T}\right) = \hat{\boldsymbol{Q}}^{\rm T}(\boldsymbol{K},t), \tag{31}$$

$$-|\boldsymbol{K}|^2\left[\ddot{\hat{\xi}} + 2\frac{\dot{a}}{a}\dot{\hat{\xi}} - 4\pi G\rho_{\rm b}\hat{\xi} + \frac{1}{a^2}\frac{{\rm d}P}{{\rm d}\rho}(\rho_{\rm b})|\boldsymbol{K}|^2\hat{\xi}\right] = \hat{Q}(\boldsymbol{K},t). \tag{32}$$

The solutions are formally written as

$$\hat{\boldsymbol{\xi}}^{\mathrm{T}}(\boldsymbol{K},t)=\frac{1}{|\boldsymbol{K}|^2}\int^t \mathrm{d}t' G^{\mathrm{T}}(t,t')\hat{\boldsymbol{Q}}^{\mathrm{T}}(\boldsymbol{K},t'), \tag{33}$$

$$\hat{\xi}(\boldsymbol{K},t)=-\frac{1}{|\boldsymbol{K}|^2}\int^t \mathrm{d}t' G(\boldsymbol{K},t,t')\hat{Q}(\boldsymbol{K},t'), \tag{34}$$

by using the Green functions $G^{\mathrm{T}}(t,t')$ and $G(\boldsymbol{K},t,t')$. The Green function $G^{\mathrm{T}}(t,t')$ does not depend on an equation of state and is given as

$$G^{\mathrm{T}}(t,t')=3(t'-t^{-1/3}t'^{4/3}), \tag{35}$$

while the Green function $G(\boldsymbol{K},t,t')$ does depend on an equation of state. Under the assumption $P=\kappa\rho^{\gamma}$, if $\gamma\neq 4/3$ and $\nu=5/(8-6\gamma)$ is not an integer, we have

$$G(\boldsymbol{K},t,t')=-\frac{\pi}{2\sin\nu\pi}\left(-\gamma+\frac{4}{3}\right)^{-1}t^{-1/6}t'^{7/6}[J_{-\nu}(A|\boldsymbol{K}|t^{-\gamma+4/3})J_{\nu}(A|\boldsymbol{K}|t'^{-\gamma+4/3})-J_{\nu}(A|\boldsymbol{K}|t^{-\gamma+4/3})J_{-\nu}(A|\boldsymbol{K}|t'^{-\gamma+4/3})], \tag{36}$$

and, if $\gamma=4/3$,

$$G(\boldsymbol{K},t,t')=-\frac{1}{2}\left(\frac{25}{36}-B|\boldsymbol{K}|^2\right)^{-1/2}t^{-1/6}t'^{7/6}\left(t^{-\sqrt{25/36-B|\boldsymbol{K}|^2}}t'^{\sqrt{25/36-B|\boldsymbol{K}|^2}}-t^{\sqrt{25/36-B|\boldsymbol{K}|^2}}t'^{-\sqrt{25/36-B|\boldsymbol{K}|^2}}\right). \tag{37}$$

In order to present the explicit form of the second-order solutions, we must compute the Fourier-transformed source terms $\hat{\boldsymbol{Q}}^{\mathrm{T}}$ and $\hat{Q}$. Hereafter we neglect the first-order transverse part $\boldsymbol{S}^{\mathrm{T}}$ in $\hat{\boldsymbol{Q}}^{\mathrm{T}}$ and $\hat{Q}$ for simplicity. This is equivalent to paying no attention to the effect of vorticity in the second-order solutions. They are written in the following convolution form:

$$\begin{aligned}\hat{\boldsymbol{Q}}^{\mathrm{T}}(\boldsymbol{K},t)=&-\frac{\mathrm{i}}{(2\pi)^3}\frac{1}{a^2}\frac{\mathrm{d}P}{\mathrm{d}\rho}(\rho_{\mathrm{b}})\int_{-\infty}^{\infty}\mathrm{d}^3\boldsymbol{K}'\hat{S}(\boldsymbol{K}',t)\hat{S}(\boldsymbol{K}-\boldsymbol{K}',t)|\boldsymbol{K}-\boldsymbol{K}'|^2\boldsymbol{K}'\cdot(\boldsymbol{K}-\boldsymbol{K}')\cdot\{\boldsymbol{K}'[\boldsymbol{K}'\cdot(\boldsymbol{K}-\boldsymbol{K}')]+\boldsymbol{K}'|\boldsymbol{K}-\boldsymbol{K}'|^2-(\boldsymbol{K}-\boldsymbol{K}')|\boldsymbol{K}'|^2\\&-(\boldsymbol{K}-\boldsymbol{K}')[\boldsymbol{K}'\cdot(\boldsymbol{K}-\boldsymbol{K}')]\},\end{aligned} \tag{38}$$

$$\begin{aligned}\hat{Q}(\boldsymbol{K},t)=&\frac{1}{(2\pi)^3}\int_{-\infty}^{\infty}\mathrm{d}^3\boldsymbol{K}'\hat{S}(\boldsymbol{K}',t)\hat{S}(\boldsymbol{K}-\boldsymbol{K}',t)\left[2\pi G\rho_{\mathrm{b}}\{[\boldsymbol{K}'\cdot(\boldsymbol{K}-\boldsymbol{K}')]^2-|\boldsymbol{K}'|^2|\boldsymbol{K}-\boldsymbol{K}'|^2\}+\frac{1}{a^2}\frac{\mathrm{d}P}{\mathrm{d}\rho}(\rho_{\mathrm{b}})\right.\\&\times\{|\boldsymbol{K}'|^2|\boldsymbol{K}-\boldsymbol{K}'|^2\boldsymbol{K}'\cdot(\boldsymbol{K}-\boldsymbol{K}')+[\boldsymbol{K}'\cdot(\boldsymbol{K}-\boldsymbol{K}')]^3+2|\boldsymbol{K}-\boldsymbol{K}'|^2[\boldsymbol{K}'\cdot(\boldsymbol{K}-\boldsymbol{K}')]^2\}\\&\left.+\frac{1}{a^2}\frac{\mathrm{d}^2P}{\mathrm{d}\rho^2}(\rho_{\mathrm{b}})\rho_{\mathrm{b}}[|\boldsymbol{K}'|^2|\boldsymbol{K}-\boldsymbol{K}'|^4+|\boldsymbol{K}'|^2|\boldsymbol{K}-\boldsymbol{K}'|^2\boldsymbol{K}'\cdot(\boldsymbol{K}-\boldsymbol{K}')]\right].\end{aligned} \tag{39}$$

Using the first-order solution (29), we obtain

$$\begin{aligned}\hat{\boldsymbol{\xi}}^{\mathrm{T}}(\boldsymbol{K},t)=&-\frac{\mathrm{i}}{(2\pi)^3}\frac{1}{|\boldsymbol{K}|^2}\int_{-\infty}^{\infty}\mathrm{d}^3\boldsymbol{K}'E^{\mathrm{T}}(\boldsymbol{K},\boldsymbol{K}',t)[C^{+}(\boldsymbol{K}')C^{+}(\boldsymbol{K}-\boldsymbol{K}')+C^{+}(\boldsymbol{K}')C^{-}(\boldsymbol{K}-\boldsymbol{K}')+C^{-}(\boldsymbol{K}')C^{+}(\boldsymbol{K}-\boldsymbol{K}')\\&+C^{-}(\boldsymbol{K}')C^{-}(\boldsymbol{K}-\boldsymbol{K}')]|\boldsymbol{K}-\boldsymbol{K}'|^2\boldsymbol{K}'\cdot(\boldsymbol{K}-\boldsymbol{K}')\{\boldsymbol{K}'[\boldsymbol{K}'\cdot(\boldsymbol{K}-\boldsymbol{K}')]+\boldsymbol{K}'|\boldsymbol{K}-\boldsymbol{K}'|^2-(\boldsymbol{K}-\boldsymbol{K}')|\boldsymbol{K}'|^2-(\boldsymbol{K}-\boldsymbol{K}')[\boldsymbol{K}'\cdot(\boldsymbol{K}-\boldsymbol{K}')]\},\end{aligned} \tag{40}$$

$$\begin{aligned}\hat{\xi}(\boldsymbol{K},t)=&-\frac{1}{(2\pi)^3}\frac{1}{|\boldsymbol{K}|^2}\int_{-\infty}^{\infty}\mathrm{d}^3\boldsymbol{K}'[C^{+}(\boldsymbol{K}')C^{+}(\boldsymbol{K}-\boldsymbol{K}')+C^{+}(\boldsymbol{K}')C^{-}(\boldsymbol{K}-\boldsymbol{K}')+C^{-}(\boldsymbol{K}')C^{+}(\boldsymbol{K}-\boldsymbol{K}')\\&+C^{-}(\boldsymbol{K}')C^{-}(\boldsymbol{K}-\boldsymbol{K}')][E(\boldsymbol{K},\boldsymbol{K}',t)\{[\boldsymbol{K}'\cdot(\boldsymbol{K}-\boldsymbol{K}')]^2-|\boldsymbol{K}'|^2|\boldsymbol{K}-\boldsymbol{K}'|^2\}+F_1(\boldsymbol{K},\boldsymbol{K}',t)\{|\boldsymbol{K}'|^2|\boldsymbol{K}-\boldsymbol{K}'|^2\boldsymbol{K}'\cdot(\boldsymbol{K}-\boldsymbol{K}')\\&+[\boldsymbol{K}'\cdot(\boldsymbol{K}-\boldsymbol{K}')]^3+2|\boldsymbol{K}-\boldsymbol{K}'|^2[\boldsymbol{K}'\cdot(\boldsymbol{K}-\boldsymbol{K}')]^2\}+F_2(\boldsymbol{K},\boldsymbol{K}',t)[|\boldsymbol{K}'|^2|\boldsymbol{K}-\boldsymbol{K}'|^4+|\boldsymbol{K}'|^2|\boldsymbol{K}-\boldsymbol{K}'|^2\boldsymbol{K}'\cdot(\boldsymbol{K}-\boldsymbol{K}')]],\end{aligned} \tag{41}$$

where the time-dependent factors are given as

$$E^{\mathrm{T}}(\boldsymbol{K},\boldsymbol{K}',t)=\int^t\frac{\mathrm{d}t'}{a^2(t')}\frac{\mathrm{d}P}{\mathrm{d}\rho}(\rho_{\mathrm{b}}(t'))G^{\mathrm{T}}(t,t')[D^+(\boldsymbol{K}',t')D^+(\boldsymbol{K}-\boldsymbol{K}',t')+D^+(\boldsymbol{K}',t')D^-(\boldsymbol{K}-\boldsymbol{K}',t')+D^-(\boldsymbol{K}',t')D^+(\boldsymbol{K}-\boldsymbol{K}',t')$$
$$+D^-(\boldsymbol{K}',t')D^-(\boldsymbol{K}-\boldsymbol{K}',t')], \tag{42}$$

$$E(\boldsymbol{K},\boldsymbol{K}',t)=\int^t\mathrm{d}t'2\pi G\rho_{\mathrm{b}}(t')G(\boldsymbol{K},t,t')[D^+(\boldsymbol{K}',t')D^+(\boldsymbol{K}-\boldsymbol{K}',t')+D^+(\boldsymbol{K}',t')D^-(\boldsymbol{K}-\boldsymbol{K}',t')+D^-(\boldsymbol{K}',t')D^+(\boldsymbol{K}-\boldsymbol{K}',t')$$
$$+D^-(\boldsymbol{K}',t')D^-(\boldsymbol{K}-\boldsymbol{K}',t')], \tag{43}$$

$$F_1(\boldsymbol{K},\boldsymbol{K}',t)=\int^t\frac{\mathrm{d}t'}{a^2(t')}\frac{\mathrm{d}P}{\mathrm{d}\rho}(\rho_{\mathrm{b}}(t'))G(\boldsymbol{K},t,t')[D^+(\boldsymbol{K}',t')D^+(\boldsymbol{K}-\boldsymbol{K}',t')+D^+(\boldsymbol{K}',t')D^-(\boldsymbol{K}-\boldsymbol{K}',t')+D^-(\boldsymbol{K}',t')D^+(\boldsymbol{K}-\boldsymbol{K}',t')$$
$$+D^-(\boldsymbol{K}',t')D^-(\boldsymbol{K}-\boldsymbol{K}',t')], \tag{44}$$

$$F_2(\boldsymbol{K},\boldsymbol{K}',t)=\int^t\frac{\mathrm{d}t'}{a^2(t')}\frac{\mathrm{d}^2P}{\mathrm{d}\rho^2}(\rho_{\mathrm{b}}(t'))\rho_{\mathrm{b}}(t')G(\boldsymbol{K},t,t')[D^+(\boldsymbol{K}',t')D^+(\boldsymbol{K}-\boldsymbol{K}',t')+D^+(\boldsymbol{K}',t')D^-(\boldsymbol{K}-\boldsymbol{K}',t')+D^-(\boldsymbol{K}',t')D^+(\boldsymbol{K}-\boldsymbol{K}',t')$$
$$+D^-(\boldsymbol{K}',t')D^-(\boldsymbol{K}-\boldsymbol{K}',t')]. \tag{45}$$

The convolution in the solutions (40) and (41) represents mode couplings in $\boldsymbol{K}$ space, which inevitably occur at second order as a result of the non-linearity. Although it is cumbersome to perform the integration in equations (42)–(45) in general, it is easy to do so if the equation of state is $P=\kappa\rho^{4/3}$. In this case, if only the $D^+(\boldsymbol{K}',t)D^+(\boldsymbol{K}-\boldsymbol{K}',t)$ part is considered, equations (42)–(45) become

$$E^{\mathrm{T}}(\boldsymbol{K},\boldsymbol{K}',t)=\frac{Bt^{\,-1/3+b(\boldsymbol{K}')+b(\boldsymbol{K}-\boldsymbol{K}')}}{\left[-\frac{1}{3}+b(\boldsymbol{K}')+b(\boldsymbol{K}-\boldsymbol{K}')\right][b(\boldsymbol{K}')+b(\boldsymbol{K}-\boldsymbol{K}')]}, \tag{46}$$

$$E(\boldsymbol{K},\boldsymbol{K}',t)=\frac{t^{\,-1/3+b(\boldsymbol{K}')+b(\boldsymbol{K}-\boldsymbol{K}')}}{3\left[-\frac{1}{6}-b(\boldsymbol{K})+b(\boldsymbol{K}')+b(\boldsymbol{K}-\boldsymbol{K}')\right]\left[-\frac{1}{6}+b(\boldsymbol{K})+b(\boldsymbol{K}')+b(\boldsymbol{K}-\boldsymbol{K}')\right]}, \tag{47}$$

$$F_1(\boldsymbol{K},\boldsymbol{K}',t)=\frac{Bt^{\,-1/3+b(\boldsymbol{K}')+b(\boldsymbol{K}-\boldsymbol{K}')}}{\left[-\frac{1}{6}-b(\boldsymbol{K})+b(\boldsymbol{K}')+b(\boldsymbol{K}-\boldsymbol{K}')\right]\left[-\frac{1}{6}+b(\boldsymbol{K})+b(\boldsymbol{K}')+b(\boldsymbol{K}-\boldsymbol{K}')\right]}, \tag{48}$$

$$F_2(\boldsymbol{K},\boldsymbol{K}',t)=\frac{Bt^{\,-1/3+b(\boldsymbol{K}')+b(\boldsymbol{K}-\boldsymbol{K}')}}{3\left[-\frac{1}{6}-b(\boldsymbol{K})+b(\boldsymbol{K}')+b(\boldsymbol{K}-\boldsymbol{K}')\right]\left[-\frac{1}{6}+b(\boldsymbol{K})+b(\boldsymbol{K}')+b(\boldsymbol{K}-\boldsymbol{K}')\right]}, \tag{49}$$

where $b(\boldsymbol{K})=\sqrt{25/36-B|\boldsymbol{K}|^2}$. Note that all these factors have the same temporal dependence, $t^{\,-1/3+b(\boldsymbol{K}')+b(\boldsymbol{K}-\boldsymbol{K}')}$. Of course, it is not a general property of the second-order solutions, but $F_1(\boldsymbol{K},\boldsymbol{K}',t)$ and $F_2(\boldsymbol{K},\boldsymbol{K}',t)$ always have the same temporal dependence as long as the equation of state is of the form $P=\kappa\rho^{\gamma}$.

4 ILLUSTRATION IN A ONE-DIMENSIONAL MODEL

In this section, we present illustrative examples of computation by the Lagrangian perturbation theory formulated in the previous section. We compute the power spectra of density perturbations by the Eulerian linear theory, and by the Lagrangian first-order and second-order approximations in a one-dimensional model, and then clarify the difference between the Eulerian and the Lagrangian approximations. In the linear regime $|\delta|\ll 1$, the Eulerian and Lagrangian approximations give the same results. However, when these approximations are extrapolated into the non-linear regime, their results do not always coincide.

In the pressureless case, the first-order approximation (i.e. the Zel'dovich approximation) coincides with the exact solution in the one-dimensional model. Although this does not hold in the presence of pressure in general, we discuss whether the Lagrangian perturbative approximations may provide a nearly exact description in the weakly non-linear regime $|\delta|\lesssim 1$, by consulting the difference between the first-order and the second-order approximations. Of course, we cannot say that one-dimensional examples are realistic, but they are instructive to show the advantages and features of non-linearity that the Lagrangian perturbation theory involves.

4.1 Equations and perturbative solutions in a one-dimensional model

First we present the basic equations and perturbative solutions in a one-dimensional model. In the Eulerian linear approximation, the density

contrast satisfies equation (27), that is

$$\frac{\partial^2\delta_{\rm lin}(k,t)}{\partial t^2}+2\frac{\dot a}{a}\frac{\partial\delta_{\rm lin}(k,t)}{\partial t}-4\pi G\rho_{\rm b}\delta_{\rm lin}(k,t)+\frac{1}{a^2}\frac{{\rm d}P}{{\rm d}\rho}(\rho_{\rm b})k^2\delta_{\rm lin}(k,t)=0, \tag{50}$$

where k is the first component of the Eulerian wavevector $\boldsymbol{k}$. We find from this equation that density perturbations whose wavenumbers are smaller than

$$k_{\rm J}\equiv\left(\frac{4\pi G\rho_{\rm b}a^2}{{\rm d}P/{\rm d}\rho}\right)^{1/2}$$

will grow to form inhomogeneous structures, and those whose wavenumbers are larger than $k_{\rm J}$ will decay with acoustic oscillations (the Jeans condition). In particular, we immediately see the behaviour of density perturbations in the case $P=\kappa\rho^{4/3}$, where the solutions of equation (50) are

$$\delta_{\rm lin}(k,t)\propto t^{-1/6\pm\sqrt{25/36-Bk^2}}, \tag{51}$$

and $k_{\rm J}=\sqrt{2/(3B)}$. If $k<k_{\rm J}$, one of the solutions becomes a growing solution; whereas if $k>k_{\rm J}$, both of the solutions are decaying ones.

The relation between the Eulerian and the Lagrangian coordinates, equation (7), in a one-dimensional model can be written as

$$\begin{cases}x_1=q_1+s_1(q_1,t),\\ x_2=q_2,\\ x_3=q_3,\end{cases} \tag{52}$$

and the energy density, equation (8), is then

$$\rho(q_1,t)=\frac{\rho_{\rm b}(t)}{1+s_{1,1}(q_1,t)}, \tag{53}$$

because the Jacobian $J=1+s_{1,1}$. The relation between $\nabla_{\boldsymbol{x}}$ and $\nabla_{\boldsymbol{q}}$, equation (12), becomes

$$\frac{\partial}{\partial x_1}=\frac{1}{J}\frac{\partial}{\partial q_1},\qquad \frac{\partial}{\partial x_2}=\frac{\partial}{\partial q_2},\qquad \frac{\partial}{\partial x_3}=\frac{\partial}{\partial q_3}. \tag{54}$$

Hence from equation (11) we have

$$\frac{1}{J}\frac{\partial}{\partial q_1}\left(\ddot s_1+2\frac{\dot a}{a}\dot s_1-\frac{1}{a^2}\frac{{\rm d}P}{{\rm d}\rho}J^{-2}J_{,1}\right)=-4\pi G\rho_{\rm b}(J^{-1}-1), \tag{55}$$

which can be reduced to

$$\ddot s_1+2\frac{\dot a}{a}\dot s_1-4\pi G\rho_{\rm b}s_1-\frac{1}{a^2}\frac{{\rm d}P}{{\rm d}\rho}\frac{s_{1,11}}{(1+s_{1,1})^2}=0 \tag{56}$$

by imposing the appropriate boundary conditions. If we assume that the equation of state is of the form $P=\kappa\rho^\gamma$, we obtain by using equation (53),

$$\ddot s_1+2\frac{\dot a}{a}\dot s_1-4\pi G\rho_{\rm b}s_1-\frac{\kappa\gamma\rho_{\rm b}^{\gamma-1}}{a^2}\frac{s_{1,11}}{(1+s_{1,1})^{1+\gamma}}=0. \tag{57}$$

It seems to be difficult to solve equation (56) or (57) exactly in general, although Götz (1988) solved it in the case $P\propto\rho$ without cosmic expansion. Thus, we consider their solutions in a perturbative manner and adopt the perturbation solutions obtained in the previous section. Note that the displacement vector $\boldsymbol{s}=(s_1,0,0)$ consists only of the longitudinal parts ($S_{,1}$, $\zeta_{,1}$, …), because the transverse parts ($\boldsymbol{S}^{\rm T}$, $\boldsymbol{\zeta}^{\rm T}$, …) vanish in a one-dimensional model. The perturbation solutions (29) and (41) become

$$\hat S(K,t)=D^+(K,t)C^+(K)+D^-(K,t)C^-(K), \tag{58}$$

$$\begin{aligned}\hat\zeta(K,t)=&-\frac{1}{2\pi K}\int_{-\infty}^{\infty}{\rm d}K'[C^+(K')C^+(K-K')+C^+(K')C^-(K-K')+C^-(K')C^+(K-K')+C^-(K')C^-(K-K')]\cdot[2F_1(K,K',t)\\ &+F_2(K,K',t)]K'^2(K-K')^3,\end{aligned} \tag{59}$$

where K is the first component of the Lagrangian wavevector $\boldsymbol{K}$. The part proportional to $E(\boldsymbol{K},\boldsymbol{K}',t)$ in the second-order solutions (41) does not appear in the above expression because it vanishes in a one-dimensional model.

In order to simplify the perturbation solutions further, let us consider the case where the equation of state is $P=\kappa\rho^{4/3}$. Although the validity of this assumption is not clear, it would be useful to understand features of the perturbation theory we have formulated. The temporal

factors are computed as

$$D^{\pm}(K,t) = t^{-1/6 \pm b(K)}, \tag{60}$$

$$2F_1(K,K',t) + F_2(K,K',t) = \frac{7}{3}\frac{Bt^{-1/3+b(K')+b(K-K')}}{\left[-\frac{1}{6} - b(K) + b(K') + b(K-K')\right]\left[-\frac{1}{6} + b(K) + b(K') + b(K-K')\right]}, \tag{61}$$

where we again take into account only the $D^{+}(K')D^{+}(K-K')$ part to compute $2F_1 + F_2$.

4.2 Initial conditions

We consider setting the initial conditions for illustration. Initial conditions for two independent physical quantities are needed to determine $C^{\pm}(K)$. Here we impose the initial conditions for the density contrast δ and the peculiar velocity $\boldsymbol{v}$, whose initial values are denoted by $\delta_{\rm in}$ and $\boldsymbol{v}_{\rm in}$, respectively. For comparison with the pressureless case, we take $\delta_{\rm in}$ and $\boldsymbol{v}_{\rm in}$ as given by the Zel'dovich approximation, which is a subclass of the first-order approximation for a pressureless fluid and becomes an exact solution in the one-dimensional model. By setting the conditions in this way, the $C^{\pm}(K)$ are expressed in terms of only $\delta_{\rm in}$, because the Zel'dovich approximation includes just one arbitrary spatial function, through which we can make a relation between $\delta_{\rm in}$ and $\boldsymbol{v}_{\rm in}$. The one-dimensional Zel'dovich approximation is written as

$$\begin{cases} x_1 = q_1 + t^{2/3}\Psi_{,1}(q_1), \\ x_2 = q_2, \\ x_3 = q_3, \end{cases} \tag{62}$$

$$\rho(q_1,t) = \frac{\rho_{\rm b}(t)}{1 + t^{2/3}\Psi_{,11}(q_1)}, \tag{63}$$

where $\Psi(q_1)$ is an arbitrary spatial function, describing initial inhomogeneity. From these equations, we have

$$\delta_{\rm in}(q_1) = \frac{1}{1 + t^{2/3}\Psi_{,11}(q_1)} - 1\Bigg|_{t=t_{\rm in}} \simeq -\Psi_{,11}(q_1), \tag{64}$$

$$\boldsymbol{v}_{\rm in}(q_1) = \left(\frac{2}{3}t^{1/3}\Psi_{,1}(q_1), 0, 0\right)\Bigg|_{t=t_{\rm in}} = \left(\frac{2}{3}\Psi_{,1}(q_1), 0, 0\right), \tag{65}$$

where we define an initial time $t_{\rm in} \equiv 1$. On the other hand, the first-order solution in the case $P = \kappa\rho^{4/3}$ gives

$$\hat{\delta}_{\rm in}(K) = K^2[C^{+}(K) + C^{-}(K)], \tag{66}$$

$$\hat{\boldsymbol{v}}_{\rm in}(K) = \left(\mathrm{i}K\left\{\left[-\frac{1}{6} + b(K)\right]C^{+}(K) + \left[-\frac{1}{6} - b(K)\right]C^{-}(K)\right\}, 0, 0\right). \tag{67}$$

Comparing equations (64), (65), (66), and (67), we obtain

$$C^{\pm}(K) = \frac{\hat{\delta}_{\rm in}(K)}{2K^2}\left[1 \pm \frac{5}{6b(K)}\right]. \tag{68}$$

Thus $C^{\pm}(K)$ are completely determined if $\hat{\delta}_{\rm in}(K)$ is provided in some appropriate manner. In our illustration, we choose $\hat{\delta}_{\rm in}(K) = |\hat{\delta}_{\rm in}(K)|\exp(\mathrm{i}\phi_K)$ so that $|\hat{\delta}_{\rm in}(K)|^2 \propto |K|^n$, where n is a spectral index, and the phases ϕ_K are randomly distributed on the interval $[0, 2\pi]$. This choice is a simplification of the Gaussian statistics for initial density perturbations $\delta_{\rm in}(q_1)$ in real space (Coles & Lucchin 1995), which is usually adopted in the study of large-scale structure formation.

4.3 Evolution of power spectra of density perturbations

Now we compute the power spectra $\mathcal{P}(|k|,t) = \mathcal{P}(k,t) \equiv \langle|\delta(k,t)|^2\rangle$ of density perturbations, where $\langle\cdot\rangle$ denotes an ensemble average over the entire distribution, by using the Lagrangian perturbation theory formulated in the preceding section. We also compute them by the Eulerian linear theory and compare the results to clarify the difference between the Eulerian and the Lagrangian perturbative approximations. In the Lagrangian approximations, we need some computation to obtain the power spectra, although the Eulerian approximation yields them directly. The procedure of the computation is the following:

(i) First we specify the initial conditions as we mentioned above. Then we have the complete form of the perturbation solutions in K space.
(ii) Next we transform the perturbation solutions in K space into those in q space via inverse Fourier transformation.
(iii) From the perturbation solutions in q space, we immediately find the density perturbations in q space by equation (53).

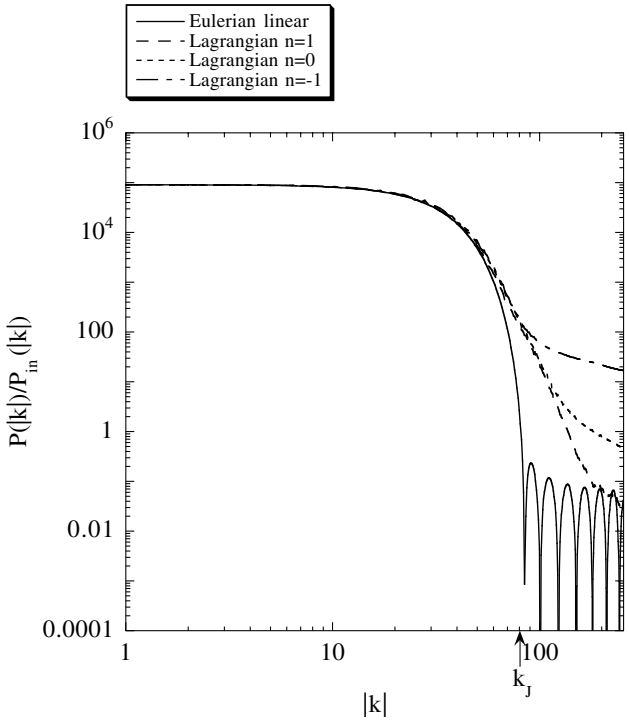

Figure 1. The 'transfer function' of density perturbations at $a = 300$ computed from the Eulerian linear theory and the Lagrangian first-order approximations. It does not depend on the initial conditions in the Eulerian linear theory, but does do so in the Lagrangian approximation.

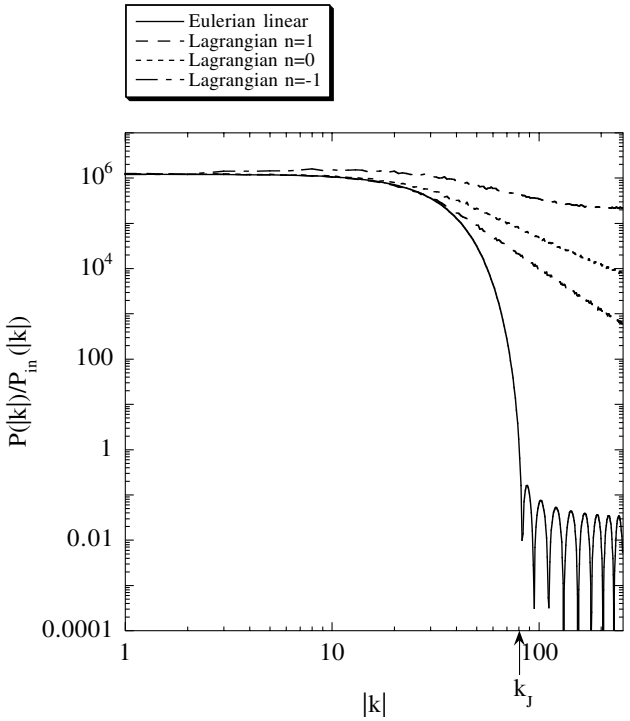

Figure 2. Same as in Fig. 1, but for $a = 1100$.

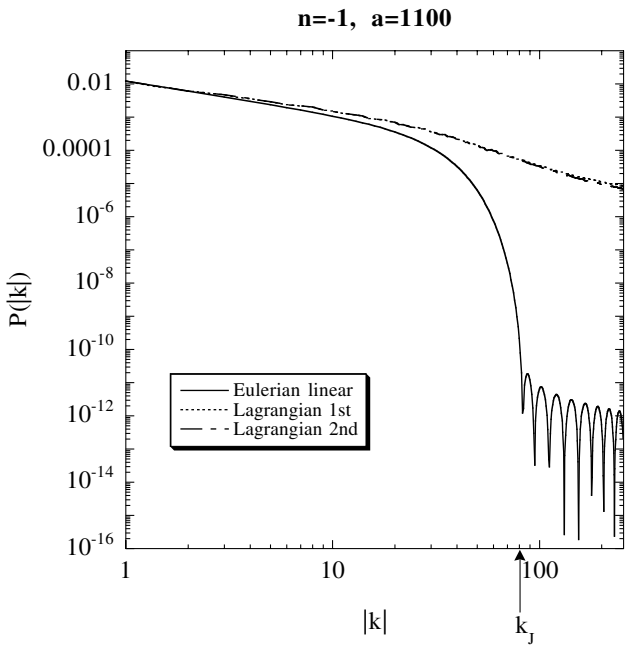

Figure 3. Power spectra of density perturbations at $a = 1100$ computed from the Eulerian linear theory, and the Lagrangian first-order and second-order approximations. The spectral index is $n = -1$.

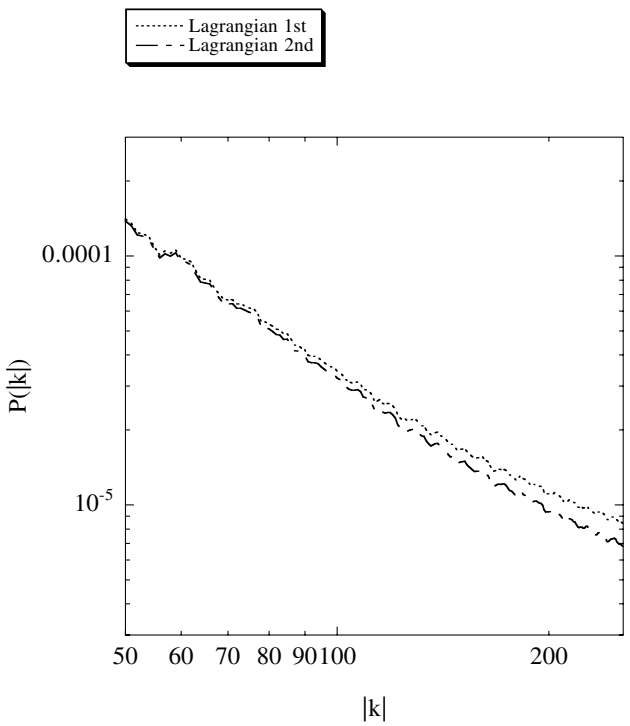

Figure 4. Power spectra at $a = 1100$ for $n = -1$, showing the small difference between the results by the first-order and the second-order Lagrangian approximations. The spectrum by the Eulerian linear approximation is omitted.

(iv) We evaluate the density perturbations in x space from those in q space.

(v) Finally, by Fourier transformation with respect to x, we obtain the power spectra of density perturbations.

By way of this procedure, we obtain the power spectra of density perturbations presented in Figs 1–4. We choose the spectral index as $n = +1, 0$ and -1. The constant B, which is proportional to κ and thus provides the strength of the pressure effect, is put in by hand. Here it is chosen so that the Jeans wavenumber $k_{\rm J} = \sqrt{2/(3B)}$ is 80. Note that $k_{\rm J}$ is now a constant because of our choice of the polytropic index $\gamma = 4/3$, although $k_{\rm J}$ depends on time in general. We set the initial conditions at $a = 1$, and pursue the evolution up to $a = 1100$.

Indeed, for all the cases $n = +1, 0$ and -1, shell crossing will occur at $a \sim 1100$ in the Lagrangian approximations despite the presence of the pressure effect. (In other words, we normalize the amplitude of the initial density fluctuations so that shell crossing occurs at $a \sim 1100$ in the Lagrangian approximations.) Then we cannot follow the evolution so deeply into the non-linear regime, as long as we consider the stages before the occurrence of shell crossing. In fact, in the illustration, $\mathcal{P}(|k|) \sim 10^{-4}$–$10^{-5}$ at $a = 300$, and $\mathcal{P}(|k|) \sim 10^{-3}$–$10^{-4}$ at $a = 1100$. Hence we must say that density perturbations remain in the weakly non-linear regime (or in the linear regime), rather than in the non-linear regime, through this illustration.

Figs 1 and 2 show our results obtained by the Eulerian linear theory and the Lagrangian first-order approximation, in terms of the 'transfer function', $\mathcal{P}(|k|, t)/\mathcal{P}_{\rm in}(|k|)$. It is convenient to use this because it does not depend on the initial conditions in the Eulerian linear theory, which actually yields

$$\frac{\mathcal{P}_{\rm lin}(|k|, t)}{\mathcal{P}_{\rm in}(|k|)} = \frac{1}{4}\left|\left[1 + \frac{5}{6b(k)}\right]D^{+}(k, t) + \left[1 - \frac{5}{6b(k)}\right]D^{-}(k, t)\right|^2. \tag{69}$$

In the Lagrangian approximations, however, it generally depends on the initial conditions. We do not present in Figs 1 and 2 the results by the Lagrangian second-order approximation, because they are almost coincident with those by the first-order one. To show the difference between the Lagrangian first-order and second-order approximations, we show in Figs 3 and 4 the power spectra at $a = 1100$ for $n = -1$, where the difference is largest within our calculations.

First we observe the results by the Eulerian linear theory. The power spectra presented in Figs 1 and 2 show the very behaviour of linear density perturbations stated in Section 4.1, i.e. density perturbations with wavenumbers $|k| < k_{\rm J}$ grow while those with wavenumbers $|k| > k_{\rm J}$ decay with acoustic oscillation. On the other hand, in the Lagrangian approximations, the shape of the curves is manifestly different from that in the Eulerian linear theory. Although there is little difference on large scales ($|k| < k_{\rm J}$), we see that the amplitude on small scales ($|k| > k_{\rm J}$) in the Lagrangian approximations is larger than that in the Eulerian linear theory. This fact has been observed also in the pressureless case (Schneider & Bartelmann 1995). The difference is small at $a = 300$, but becomes larger as time proceeds. Comparing the Lagrangian first-order and second-order approximations in Fig. 3, they are found to give almost coincident results through our computation from $a = 1$ to $a = 1100$, and we can hardly observe any difference between them. We present the enlarged power spectra in Fig. 4, where the difference is barely visible. Indeed the difference is less than 10 per cent at $|k| \lesssim 150$. In the second-order approximation, however, the amplitude of the power spectrum is slightly suppressed, compared with the first-order one. The features of the power spectra mentioned above are common for all the cases, $n = +1, 0$ and -1.

4.4 Discussion of the power spectra

Let us consider the reasons for the features of the power spectra. First we examine the difference between the Eulerian and the Lagrangian approximations, which has been discussed in the pressureless case by Schneider & Bartelmann (1995). In the Eulerian linear theory, density perturbations with a wave mode evolve without being influenced by those with another mode. In the Lagrangian approximations, however, non-linearities are induced in the calculation of density perturbations. The origin of such non-linearity lies in the expression of the density contrast in the Lagrangian description as well as in the transformation of the density contrast in Lagrangian coordinates $\boldsymbol{q}$ into those in Eulerian coordinates $\boldsymbol{x}$. To see this fact, let us express the Lagrangian density perturbations in Eulerian coordinates in a one-dimensional system within a perturbative manner. The relation between $\boldsymbol{x}$ and $\boldsymbol{q}$ is given as

$$x_1 = q_1 + s_1(q_1, t),$$

where we assume that s_1 is small enough to be treated as a perturbation. Using this relation iteratively, the inverse relation is obtained as

$$q_1 = x_1 - s_1(q_1, t) = x_1 - s_1(x_1, t) + O((s_1)^2).$$

Then we have

$$s_1(q_1, t) = s_1(x_1, t) - \frac{\partial s_1(x_1, t)}{\partial x_1} s_1(x_1, t) + O((s_1)^3), \tag{70}$$

$$\frac{\partial}{\partial q_1} = \frac{\partial x_1}{\partial q_1}\frac{\partial}{\partial x_1} = \frac{\partial}{\partial x_1} + \frac{\partial s_1(q_1, t)}{\partial q_1}\frac{\partial}{\partial x_1} = \frac{\partial}{\partial x_1} + \frac{\partial s_1(x_1, t)}{\partial x_1}\frac{\partial}{\partial x_1} + \cdots. \tag{71}$$

By using equations (70) and (71), the expression for the density contrast in the Lagrangian coordinates

$$\delta_{\rm L}(q_1,t) = [1 + s_{1,1}(q_1,t)]^{-1} - 1 = -\frac{\partial s_1(q_1,t)}{\partial q_1} + \left[\frac{\partial s_1(q_1,t)}{\partial q_1}\right]^2 + O((s_1)^3)$$

(subscript 'L' denotes 'Lagrangian') is transformed to

$$\delta_{\rm L}(x_1,t) = -\frac{\partial s_1(x_1,t)}{\partial x_1} + \frac{\partial^2 s_1(x_1,t)}{\partial x_1^2} s_1(x_1,t) + \left[\frac{\partial s_1(x_1,t)}{\partial x_1}\right]^2 + O((s_1)^3), \tag{72}$$

where the first term on the right-hand side corresponds to the density contrast $\delta_{\rm lin}(x_1,t)$ in the Eulerian linear theory. Equation (72) indicates that the density contrast obtained by the Lagrangian description includes extra non-linear terms, which cause mode couplings. For example, if initial density perturbations consist of a single wave mode, $\delta_{\rm in}(x_1) \propto \sin kx_1$, such non-linear terms generate high-frequency modes such as $\sin 2kx_1$. Of course, in the Eulerian linear theory, mode couplings never occur and the existence of just a single mode is preserved, i.e. $\delta_{\rm lin}(x_1,t) \propto \sin kx_1$. To see the mode-coupling effect quantitatively, one should consider the Fourier transform of equation (72),

$$\delta_{\rm L}(k,t) = \delta_{\rm lin}(k,t) + \sum_{k' \neq k} \frac{k\delta_{\rm lin}(k',t)\delta_{\rm lin}(k-k',t)}{k-k'} + O((\delta_{\rm lin})^3), \tag{73}$$

where the second term on the right-hand side represents the mode couplings. Note that the second term is written as a summation with respect to all wavenumbers. Thus the effect of the second term may be larger than the simple square of $\delta_{\rm lin}(k,t)$ by the order of the number of wave modes. In the case of our illustration, it may be larger by two orders. For example, if the power spectrum has a peak value 10^{-4}, the mode-coupling effect can generate an amplitude of 10^{-6} at high frequency. One may wonder, at first glance at our results, why the results by the Lagrangian approximations contain such large amplitude at high frequency, although the illustration is performed in the nearly linear regime. However, this fact is explained by the effect of the mode couplings.

The appearance of the large amplitude on small scales may be interpreted physically as follows. In the Lagrangian description of hydrodynamics, one obtains physical quantities in a frame comoving with the flow lines of the fluid. If there exists a growing density enhancement in a region, one can see that the flow lines there become close to each other because of gravitational instability. In other words, one knows by following the flow lines that the physical wavelength of an inhomogeneity gets small as a result of gravitational contraction. In fact, density perturbations with an initially small wavenumber $|K|$ become those with a large $|k|$ later. This can easily be seen by the relation between K and k, given as

$$|k| \sim \frac{1}{\ell} \sim \frac{1}{L + s_1(L,t)} = \frac{1}{L}\left[1 + \frac{s_1(L,t)}{L}\right]^{-1} \sim |K|[1 + \delta(L,t)],$$

where ℓ is the physical wavelength of the inhomogeneity measured in the Eulerian coordinates, and L denotes the initial wavelength. Thus we may conclude that the appearance of the large amplitude on small scales is due to the fact that the scale of the inhomogeneity is shortened as the inhomogeneity grows because of gravitational instability.

Furthermore, let us check the behaviour of the power spectra by the Lagrangian approximations for large $|k|$. As we stated in the previous subsection, shell-crossing singularities arise in spite of the presence of the pressure effect in our perturbation scheme. In our illustration, they arise at $a \sim 1100$, and thus the epoch $a = 1100$ is just before the occurrence of shell crossing. In such an epoch, the power spectrum behaves like $\mathcal{P}(|k|) \propto |k|^{-1}$ for large $|k|$ in a one-dimensional system (Schneider & Bartelmann 1995). This behaviour concerns only the occurrence of shell crossing, and is seen not only in the Zel'dovich approximation but also in our results, Figs 2 and 3. Note that in Fig. 2, the 'transfer function' behaves like $\mathcal{P}(|k|)/\mathcal{P}_{\rm in}(|k|) \sim |k|^{-(n+1)}$ at high frequency, showing a dependence on the initial conditions, while Fig. 3 shows the behaviour directly. It should also be stressed that the above three kinds of argument on the Lagrangian power spectra hold true whether or not the pressure effect is taken into account. In this sense, it is natural that the results of Schneider & Bartelmann (1995) and ours have a similar tendency.

Next let us confirm the small difference between the first-order and second-order Lagrangian approximations. For a rough estimation, we consider perturbations with a single wave mode K so that the first-order solution in q space is written in the form

$$S(q_1,t) = \frac{\epsilon}{K^2} D(K,t) \sin Kq_1, \tag{74}$$

where ϵ denotes the amplitude of the initial density perturbations, and $D(K,t) = t^{-1/6+b(K)}$. Then the second-order solution becomes

$$\zeta(q_1,t) \sim -\frac{\epsilon^2}{4\pi K_{\rm J}^2} D(K,t)^2 \sin 2Kq_1, \tag{75}$$

where $K_{\rm J} = k_{\rm J} = \sqrt{2/(3B)}$ is a wavenumber corresponding to the Jeans length. The fraction of $S(q_1,t)$ and $\zeta(q_1,t)$ is estimated as

$$\left|\frac{\zeta(q_1,t)}{S(q_1,t)}\right| \lesssim \epsilon\left(\frac{K}{K_{\rm J}}\right)^2 D(K,t). \tag{76}$$

If $K > K_J$, the factor $D(K,t)$ decreases with time and so the fraction $|\zeta/S|$ remains small forever. In contrast, if $K \ll K_J$, the factor $D(K, t)$ increases with time, but K/K_J is small. Then the fraction $|\zeta/S|$ cannot grow to be very large at early times. Indeed, in our calculations, it is less than about 10 per cent during the period up to $a = 1100$. As time proceeds, however, $|\zeta/S|$ will become large if $K \ll K_J$. This is a simple argument, but inequality (76) may be useful to give a criterion for the effect of the second-order terms. To make this argument more rigorous, we should take into account the mode-coupling effect, as we do in equation (73). In the estimation of the second-order solution, however, it is not essential to include the mode-coupling effect. It is rather significant to notice that the right-hand side of inequality (76) has the factor $(K/K_J)^2$. The presence of this factor is because the second-order solution is of purely pressure origin in a one-dimensional model. In other words, the gravitational effect is completely included in the first-order solution in a one-dimensional model. Thus we can confirm the small difference between the first-order and second-order Lagrangian approximations. This fact tells us that the difference between the first-order approximation and the exact solution is also small, at least up to $a = 1100$. On the other hand, in the pressureless case, the first-order approximation (i.e. the Zel'dovich approximation) becomes the exact solution in a one-dimensional model, and this fact is a strong argument for the validity of the Zel'dovich approximation. In this sense, we can also expect an accurate description by the Lagrangian approximations in the weakly non-linear regime in the presence of pressure, as in the pressureless case.

5 CONCLUDING REMARKS

We have developed a perturbative approximation theory, based on the Lagrangian description of hydrodynamics in the framework of Newtonian cosmology, by extending the method of Adler & Buchert (1999). Including the 'pressure' effect of the fluid, we have derived and solved the perturbation equations in Lagrangian coordinates up to second order. In particular, we have presented an explicit form for the second-order solutions for the case $P \propto \rho^{4/3}$. We have also computed the evolution of the power spectra of density perturbations in a one-dimensional model, based on the Eulerian and Lagrangian approximations. Comparing the power spectra, we have found the difference between these approximations. In particular, a large amplitude on small scales has appeared in the results of the Lagrangian approximations beyond the linear regime. Moreover, the first-order and second-order Lagrangian approximations have been found to yield almost the same results within our calculations. Thus we can conclude that, in a one-dimensional system, the first-order Lagrangian approximation provides a nearly exact description in the weakly non-linear regime.

In the computation of the power spectra of density perturbations by the Lagrangian approximations, we have found that shell-crossing singularities occur even in the presence of the pressure effect. However, the epoch of the occurrence of shell crossing in our approximations is, of course, later than that in the Zel'dovich approximation. This fact is easily seen by considering perturbations with a single wave mode so that the first-order solution is given by equation (74) again. Then the energy density, equation (53), becomes

$$\rho(q_1, t) = \frac{\rho_b(t)}{1 - \epsilon D(K, t) \sin Kq_1}. \tag{77}$$

If $K < K_J$, the denominator on the right-hand side goes to zero in a finite time, i.e. shell crossing will occur. But, since the growth rate $D(K, t)$ is weaker than that of the Zel'dovich approximation, the shell-crossing epoch becomes later.

In this paper, we focus our attention on the case $P \propto \rho^{4/3}$, where the solutions of the perturbation equations are written in a simple form. This equation of state is nothing other than an assumption to simplify the perturbation solutions. However, the form that an effective equation of state takes is crucial when velocity dispersion is replaced with a pressure-like force. Thus, in order to make our formulation more useful, we must reconsider the equation of state that holds effectively in high-density regions, where velocity dispersion plays an important role. For example, Buchert & Domínguez (1998) found that a relation $P \propto \rho^{5/3}$ is favoured for small velocity dispersion under the kinematical restriction that the fluid motion involves no shear. Extensions of our formulation to such cases, as well as a more generic determination of the equation of state, will be the subjects of future investigations.

ACKNOWLEDGMENTS

We would like to thank the referee, Professor Bernard Jones, for constructive comments. We also thank Thomas Buchert, Kei-ichi Maeda, Hiroki Anzai and Momoko Suda for helpful discussions and many valuable remarks.

REFERENCES

Adler S., Buchert T., 1999, A&A, 343, 317
Binney J., Tremaine S., 1987, Galactic Dynamics. Princeton Univ. Press, Princeton, NJ
Bouchet F. R., Juszkiewicz R., Colombi S., Pellat R., 1992, ApJ, 394, L5
Bouchet F. R., Colombi S., Hivon E., Juszkiewicz R., 1995, A&A, 296, 575
Buchert T., 1989, A&A, 223, 9
Buchert T., 1992, MNRAS, 254, 729
Buchert T., 1994, MNRAS, 267, 811
Buchert T., Domínguez A., 1998, A&A, 335, 395
Buchert T., Ehlers J., 1993, MNRAS, 264, 375
Catelan P., 1995, MNRAS, 276, 115

Coles P., Lucchin F., 1995, Cosmology: The Origin and Evolution of Cosmic Structure. Wiley, Chichester
Coles P., Melott A. L., Shandarin S. F., 1993, MNRAS, 260, 765
Couchman H. M. P., 1999, in Miyama S. M., Tomisaka K., Hanawa T., eds, Numerical Astrophysics. Kluwer Academic, Dordrecht, p. 1
Götz G., 1988, Classical Quantum Gravity, 5, 743
Gurbatov S. N., Saichev A. I., Shandarin S. F., 1989, MNRAS, 236, 385
Hockney R. W., Eastwood J. W., 1988, Computer Simulation Using Particles. IOP Publishing, Bristol
Melott A. L., Pellman T. F., Shandarin S. F., 1994, MNRAS, 269, 626
Miyoshi K., Kihara T., 1975, PASJ, 27, 333
Munshi D., Sahni V., Starobinsky A. A., 1994, ApJ, 436, 517
Peebles P. J. E., 1980, The Large-Scale Structure of the Universe. Princeton Univ. Press, Princeton, NJ
Sahni V., Coles P., 1995, Phys. Rep., 262, 1
Sahni V., Shandarin S., 1996, MNRAS, 282, 641
Sasaki M., Kasai M., 1998, Prog. Theor. Phys., 99, 585
Schneider P., Bartelmann M., 1995, MNRAS, 273, 475
Weinberg S., 1972, Gravitation and Cosmology. Wiley, New York
Yoshisato A., Matsubara T., Morikawa M., 1998, ApJ, 498, 48
Zel'dovich Ya. B., 1970, A&A, 5, 84

This paper has been typeset from a TEX/LATEX file prepared by the author.